analytical chemistry

Article

pubs.acs.org/ac

In Vitro Selection, Characterization, and Biosensing Application of High-Affinity Cylindrospermopsin-Targeting Aptamers

Reda Elshafey,[†] Mohamed Siaj,[‡] and Mohammed Zourob*[,§,⊥]

[†]Centre – Énergie, Matériaux et Télécommunications, Institut National de la Recherche Scientifique, 1650, Boul. Lionel Boulet, Varennes (Québec), Canada J3X 1S2

[‡]Département de Chimie et Biochimie, Université du Québec à Montréal, Montréal (Québec), Canada H3C 3P8

[§]Centre of Biomedical Engineering, Cranfield University, Cranfield, Bedfordshire MK43 0AL, U.K.

[⊥]Chemistry Department, Alfaisal University, Riyadh 11533, Kingdom of Saudi Arabia

Supporting Information

ABSTRACT: Contamination of freshwater with cyanotoxin cylindrospermopsin (CYN) represents a significant global concern for public health. The sensitive detection of CYN is necessary to effectively manage and control the treatment of water resources. Here we report a novel, highly sensitive label-free aptasensor for CYN analysis, using aptamers as specific receptors. We have selected the DNA aptamers from a diverse random library using the in vitro screening SELEX approach. The aptamers exhibited high affinity for CYN with K_d of nanomolar range. One aptamer exhibited conformational change upon CYN recognition (CD analysis) and was used to fabricate the label-free impedimetric aptasensor for CYN. A self-assembled monolayer from a disulfide-derivatized aptamer was formed on a gold electrode to fabricate the aptasensor. Upon CYN capturing to the aptasensor surface, a marked drop in the electron transfer resistance was obtained, which was used as the principle of detection of CYN. This resulted from the aptamer's conformational change induced by CYN recognition. The present aptasensor could detect CYN with the limit of detection as low as 100 pM and a wide linear range of 0.1 to 80 nM. When mounted on the gold surface, the aptamer exhibited a lower dissociation constant for CYN than that observed in the fluorescence assay, implying that the anchoring of the aptamer on the Au surface improved its affinity to CYN. Moreover, the aptasensor showed high specificity toward other coexistent cyanobacterial toxins of microcystin-LR and Anatoxin-a. Further biosensor designs will be generated using those aptamers for simple and sensitive CYN monitoring.

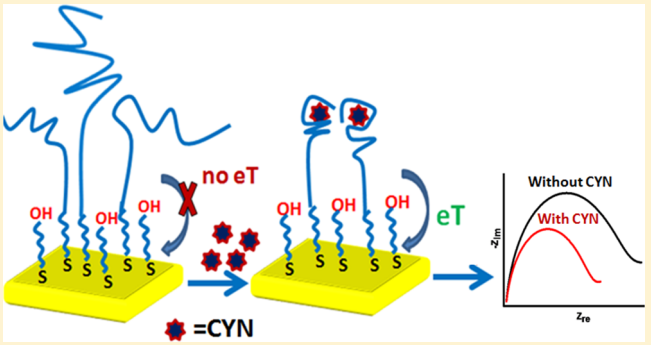

Cylindrospermopsin (CYN) is rapidly emerging as globally important cyanobacterial freshwater toxin, since the human CYN poisoning accident in 1979 (Queensland, Australia).[1] CYN is a water-soluble and heat-stable alkaloid, produced by a variety of cyanobacteria strains such as *Cylindrospermopsis raciborskii*[2] and *Anabaena bergii*.[3] CYN has two natural variants, deoxycylindrospermopsin (deoxy-CYN) and 7-epicylindrospermopsin (7-epi-CYN)[4] (see Figure S1 of the Supporting Information), which have very similar structures (the position of the hydroxyl group being the only difference). CYN and 7-epi-CYN showed similar toxicity in the mouse bioassay,[5] while the toxicity of the deoxy-CYN is still under investigation.[6] The complete loss of the uracil group from cylindrospermopsin, removes its toxicity.[7] A guideline value for safe water supply of 1 μg/L of CYN has been proposed based on toxicity studies.[8]

Hepatotoxicity is the main effect of CYN; it also affects lungs, kidneys, intestinal tract, stomach, and vascular and lymphatic systems.[9] Moreover, CYN is proved to be cytotoxic, geneotoxic,[10] dermatoxic, and a tumor promoter. Unlike microcystins, CYN is typically extracellular in water, thus, the removal of the bacteria filaments during water treatment does not remove the toxin.[11] Exposure to CYN occurs through drinking water, recreational activities, or by consuming foods, in which CYN has accumulated.

Since the recognition of the harmful impact of CYN on human health as well as wild animals, fast, simple, and accurate detection of this toxin in water bodies has been identified as an important and critical goal. Mouse bioassay is the most widely used method for estimating the toxicity of the cyanobacterial toxins.[12] However, the low sensitivity and lack of reliability, as well as the ethical problems[13] are still necessary to overcome. Thus, other alternatives are critically needed. Chromatographic methods coupled to ultraviolet[14] or mass spectrometry (LC/MS),[15] and capillary electrophoresis[16] are currently used for

Received: June 11, 2014
Accepted: August 14, 2014

   dx.doi.org/10.1021/ac502157g | *Anal. Chem.* XXXX, XXX, XXX–XXX

CYN detection. Immunoassays such as competitive enzyme-linked immunosorbent assay (ELISAs)[17] are also used for CYN assay in the LOD and concentration range of 0.04 μg/L and 0.05−2 μg/mL. However, most of these techniques are sophisticated, expensive, and not suitable for field application. They are also unsuitable for routine screenings and require highly skilled personnel. Thus, the current research focuses on developing biosensors so as to overcome the disadvantages of the other approaches. There are currently no reported biosensors for CYN because there was no commercially available antibody for CYN out of the ELISA kit. Recently, the first development of polyclonal and monoclonal antibodies to the CYN was reported.[18] Further studies on the affinity and cross reactivity are required, as well as addressing the challenges of stability and production costs. Moreover, the design of immunosensors for small molecules such as CYN will rely on competitive immunoassays, which necessitate the labeling of antibodies with enzymes as well as many assay steps. The lack of simplicity and the limited stability are important challenges that need to be addressed. Therefore, there is still an urgent need to develop novel assays to provide rapid and simple CYN monitoring in fresh water.

Aptamers are in vitro screened short ssDNA or ssRNA from random nucleic acid libraries. Aptamers can fold into special structures and possess a great ability to recognize specific targets. Since their production in 1990[19,20] as alternative biorecognition probes, aptamers offered favorable advantages over other molecular receptors. For example, they (1) can be engineered in vitro without the need of live animals, (2) can be produced and labeled by chemical synthesis at a very low cost, (3) can possess small size with high affinity, (4) most notably, are thermally stable for commercially shipping at ambient temperature, (5) can be easily modified by various functional tags to favor immobilization onto many surfaces, (6) are independent of ligand's size or type, as can be easily developed against toxins, small molecules, or even whole cells, and (7) have diversity in design of potential detection strategies.

Conformational switching by aptamers upon target recognition is commonly used for aptasensors design, as this change is accompanied by either an increase or decrease in the readout. The aptasensors signals can be monitored electrochemically,[21] by quartz crystal microbalance[22] or by surface plasmon resonance.[23] Among them, electrochemical methods are proven to be powerful analytical tools due to their high sensitivity, fast response, low cost, simple instrumentation, and the possibility of miniaturization. Up to now, few studies have been reported for the identification of aptamers targeting toxins, such as ochratoxin A[24] fumonisin B1,[25] saxitoxin,[26] and microcystin-LR.[27] However, there is no reported work regarding the aptamer screening and identification for cylindrospermopsin.

In this work, we report the first results of the in vitro selected DNA aptamers that bind specifically and tightly to the cytotoxin CNY, a water contaminant for which no aptamers have been reported to date. The selection was performed by using the approach known as systematic evolution of ligand by exponential enrichment (SELEX) to isolate high-affinity aptamers from a diverse library of 10^{15} random DNA oligonucleotides. The aptamer sequence which exhibited a structural conformational change after CYN binding was utilized for designing and constructing a simple and label-free impedimetric aptasensor for CYN.

EXPERIMENTAL SECTION

Materials and Reagents. All materials and reagents which were employed for the aptamer screening and the aptasensor fabrication are mentioned in the Supporting Information.

Preparation of Cylindrospermopsin Sepharose Beads. Initially, 100 μg of cylindrospermopsin was dissolved in 2 mL of conjugation buffer (bicarbonate buffer, pH 9.6, 0.1 M) and then added directly to 2 mL of DVS beads after washing several times with conjugation buffer. Then, the mixture was rotated overnight at room temperature. After the conjugation reaction of the CYN, the DVS activated sepharose beads via its hydroxyl groups, the beads were washed extensively with conjugation buffer, 2 min for each time, followed by adding 2 gel volume of 0.1 M Tris base to quench the unconjugated DVS groups, and stirred gently for another 2 h. Finally, the beads were washed three times, 2 min each time, with 5 vol of 0.7% w/v NaCl added to 0.05% azide w/v to remove unbound Tris. For the counter selection rounds, negative beads were prepared by adding 2 gel volumes of 0.1 M Tris base to prewashed DVS beads and equilibrated in bicarbonate buffer, pH 9.61. The coupling reaction of the CYN on the DVS beads was confirmed by performing an indirect ELISA in which the free DVS beads (blocked) were used as a control. In summary, the CYN-beads and the free ones were incubated with rabbit anti-CYN antibody (from ELISA kit) for 1 h, after washing with 0.1% Tween-PBS buffer and blocking with 1% BSA for 1 h. The beads were extensively washed, and a secondary antibody was added and incubated for another 1 h. After washing and incubating the beads for 30 min with chromogen (TMB) solution, a blue color was obtained in the toxin-coated beads; while no color was observed for the free bead, which confirms the success of the coupling reaction. Finally, the CYN-DVS beads and the negative beads (DVS) were stored in a Tris buffer, pH 7, binding buffer containing 0.02% sodium azide at 4 °C and covered with Al foil for further use.

In Vitro Selection of the DNA Aptamers. The selection of DNA aptamers against CYN, cloning and sequencing, and the determination of dissociation constant (K_d), were mentioned in detail in the Supporting Information.

Circular Dichroism (CD) Characterization. The structural conformation of DNA aptamer before and upon toxin recognition was investigated by circular dichroism spectroscopy. We employed 1 μM of the aptamer sequence CYN9, and the spectrum was measured before and after the addition of 2 μM CYN in a 1 cm path length, quartz cuvette in an optical chamber. Background signals of binding buffer and 2 μM CYN in binding buffer were recorded and subtracted from the CD spectra. All measurements were made from 230 to 340 at 0.1 nm intervals, the accumulation of three scans at 20 nm/min, with a 1 nm bandwidth, and a time constant of 1 s. The chamber was deoxygenated with dry purified nitrogen (99.99%) before use and kept in the nitrogen atmosphere during experiments. For CD measurements, to obtain a pronounced signal change, higher concentration of analyte was used to reach the saturation of the high aptamer concentration.

Aptasensor Preparation. Gold electrodes were polished to mirror smoothness successively with 1.0, 0.3, and 0.05 mm alumina slurry on a clean polishing microcloth. After each polish, the electrodes were thoroughly washed with Milli-Q water. After sonicating in water and absolute alcohol for 5 min each, the electrode was incubated with piranha solution (3:1 mixture of concentrated H_2SO_4 and 30% H_2O_2 for 5 min).

dx.doi.org/10.1021/ac502157g | Anal. Chem. XXXX, XXX, XXX−XXX

Table 1. Aptamer Sequences Selected for Characterization and Their Dissociation Constants (K_d) with CYN

group	sequence name	aptamer structure 5′-3′	K_d (nM)[a]
1	CYN4	GGCCACAACCCAACGACACTGACTGTACTGAATAATGTCTGTCAAACATCCGCGTGGTG	180.4
2	CYN17	CACCACCACAACACACGCACAGCTAGGACCGGTCGTAGGTATATCTGTTGTTCATGCGCG	57.41
3	CYN10	GGGCAACAGACACTAGTACCCGCCCGCCAGCCCCAGCATCATGCCCGTTGTGTGTGTG	NB
4	CYN9	GGCATCAGGCAACAACCGATGGTCCGGCCACCCTAACAACCAGCCCACCCACCACCCCGCCG	88.78
5	CYN19	CACAGCGTGACACGGCAACCCACCCACCAGCCCCGTCAACGACCTATACCTGTGCTGCGCA	87.4
6	CYN26	CACCAACGGACATCAGTACCCACCCGCCAGCCCCAACATCATGCCCATTCTGCGTGTCG	176.3
7	CYN2	GGGCGGCGGG GGGGTGGGCACTGACTGGTGTGGTTGCG	NB

[a]NB: not bound.

Following washing with water, the electrode was electrochemically treated by potential cycling in 0.1 M H_2SO_4, until stable typical voltammograms are obtained. After washing with water, dried by nitrogen, it is incubated into 1 μM disulfide-modified aptamer in BB for 24 h to proceed the self-assembly reaction at room temperature. Subsequently, the aptamer-modified electrode was washed with copious binding buffer to remove the nonimmobilized aptamer molecules. After exposed to a 1 mM 6-mercapto-1-hexanol (MCH) in 10 mM phosphate buffer saline, pH 7.4, for 30 min to block the remaining bare regions and minimize the density of the aptamer layer by displacing the nonspecifically adsorbed aptamer nucleotides, the resulting electrode was ready for CYN detection or kept in binding buffer solution at 4 °C until further use.

Instrumentation and Electrochemical Measurements. Alternating current (AC) impedance and cyclic voltammetric (CV) measurements were carried out in a conventional three-electrode setup using PGSTAT 302N Autolab potentiostat/galvanostat (EcoChemie, The Netherlands) which was equipped with a working electrode (1.6 mm diameter disk-shaped, aptamer modified Au electrodes, an Ag/AgCl (satd) reference electrode, and a Pt wire counter electrode. The fluorescence and UV measurements were performed using NanoDrop 3300 fluorospectrometer and NanoDrop 2000C spectrophotometer, respectively (Fisher Scientific, Canada). Circular dichroism (CD) measurements were performed by using Jasco-810 spectropolarimeter.

For CYN aptasensor recognition and the other control experiments, the aptamer-modified gold electrodes were incubated with different concentrations of CYN, microcystin-LR (MC-LR), and anatoxin-a (ATX) in BB for 100 min. After rinsing with BB to remove the nonspecifically bound toxins, it was subjected directly to record impedance spectra. For the CV experiments, a scan rate of 100 mV/s was used. The electrochemical impedance spectroscopy (EIS) spectra were recorded over a frequency range from 100 kHz to 3 Hz using an alternative voltage with an amplitude of 10 mV, superimposed on a dc potential of 0.21 V (vs a Ag/AgCl reference electrode). The impedance data were represented by Nyquist plots, which were fitted using AUTOLAB software, Nova 1.8. All measurements were performed in 10 mM PBS buffer, pH 7.4, in the presence of 5 mM $[Fe(CN)_6]^{4-/3-}$ as a redox couple.

RESULTS AND DISCUSSION

Selection of Aptamers Binding Cylindrospermopsin. Here we show the first results of aptamer identification of CYN, the cyanobacterial hepatotoxin for which there are no reported aptamers so far. We believe that our results could have great potential for the field of biosensors. By investigating the CYN structure as an alkaloid with tricyclic guanidine and sulfate ester, bridged with uracil moiety (Figure S1 of the Supporting Information), we found that the hydroxyl group of the uracil bridge is the suitable terminal moiety for coupling to the solid support. Two activated beads could be used for hydroxyl group coupling, the divinyl sulfone (DVS) and epoxy-activated sepharose beads. Conjugation of epoxy-activated beads to hydroxyls is favored at a basic pH of 11−13, which was not suitable for CYN, because of the low stability of CYN at higher pH values. However, DVS coupling reactions to the hydroxyl group could have occurred at pH values of 8−10, which can work for CYN. Therefore, DVS-activated beads were used as a solid matrix to immobilize the CYN via stable linkage to its hydroxyl groups. Such coupling will leave the other functional groups (positively charged moieties, for instance, guanidine zwitterionic structure) of the CYN molecule accessible for DNA binding during the screening, which may guarantee the success of the selection of aptamers with high affinity and specificity.[29] The free divinyl sulfone groups on the beads were blocked with Tris buffer according to the protocol to diminish the nonspecific binding DNA to the beads.

The DNA library of 10^{15} random 60- nucleotide sequences was screened against CYN-DVS beads using the SELEX approach. An increasing amount of DNA recovery was observed in the beginning of the selection, implying the enrichment of cylindrospermopsin-binding DNA (Figure S2 of the Supporting Information).

In order to increase the aptamers selectivity against CYN, counter selection using blank beads was performed. Once the DNA recovery became significantly higher than the previous round, two consecutive counter selections for CYN (after the sixth and seventh rounds) were carried out. Recovery of DNA significantly reduced in the first counter-selection, indicating the elimination of sequences that bind to the sepharose beads and not to CYN. However, we did not notice a significant drop in DNA recovery after the second counter-selection round (Figure S2 of the Supporting Information), implying that the nonspecific-bonded ssDNA sequences were eliminated.

After 12 cycles of selection, at which point a significant enrichment of cylindrospermopsin binding DNA was observed (Figure S2 of the Supporting Information), the selection cycles were stopped and the eluted DNA cloned. We noticed that the DNA recovery after the 10th round had decreased slightly, possibly due to the leaching of some CYN from the beads during the storage period.

Twenty-nine clones were picked and sent for sequencing. The identified sequences were analyzed by multiple sequence alignment using PRALINE[28] and subgrouped into 7 families according to their similarities. We observed significant consensus regions between the sequences in each group, and some sequences were in fact identical (Figure S3 of the Supporting Information). One sequence from each group was

dx.doi.org/10.1021/ac502157g | Anal. Chem. XXXX, XXX, XXX−XXX

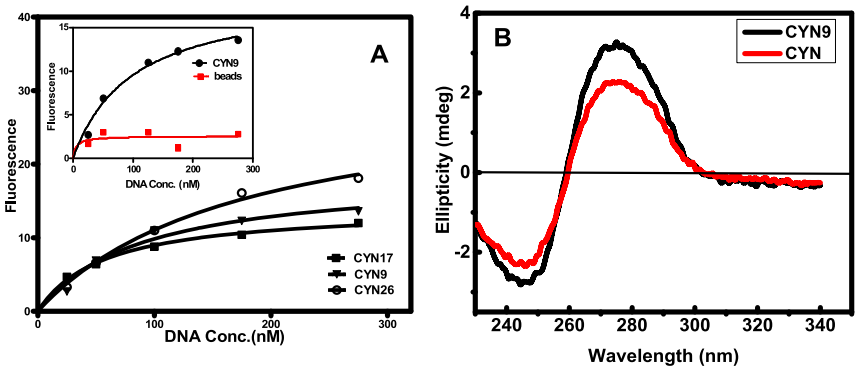

Figure 1. (A) Binding saturation curve of selected aptamers to CYN and calculation of dissociation constants (K_d) by nonlinear regression analysis. Inset the fluorescence binding assay of aptamer CYN9 with CYN-DVS beads (black curve) and negative beads (red curve). The K_d of CYN–aptamer was determined to be 88.78 nM. (B) Circular dichroism spectra of 1 μM CYN9 before (black) and after (red) recognition to 2 μM CYN at ambient temperature, with all solution in BB.

picked for further binding affinity studies with CYN, as shown in Table 1.

Binding assays were then performed to calculate the dissociation constants (K_d) using different amounts of fluorescein-labeled aptamers and a fixed amount of CYN beads. The fluorescence binding assays for some selected aptamer sequences are shown in Figure 1A. Five aptamers showed good affinity to CYN with K_d values, ranging from 57.4 to 180.4 nM, while two aptamers did not exhibit binding (Table 1).

Additionally, the binding of aptamer CYN9, which was used for biosensor fabrication, was also tested against the negative DVS sepharose beads. As shown in Figure 1A (inset), the CYN9 sequence did not exhibit any binding to negative sepharose beads, indicating the high selectivity to CYN.

Circular dichroism (CD) was employed to monitor the structural conformation change of free and target-bound forms of CYN9. As depicted in Figure 1B, the CD spectrum shows that the aptamer strand mainly forms a B-type duplex with the characteristic positive band at 278.5 nm and a negative band at about 248 nm (Figure 1B, black curve).[30] Upon adding CYN (2 μM), a significant decrease of the ellipticity at 278.5 and 248 nm was observed. This change in the CD spectra indicates the folding of the aptamer into a different conformation upon binding with CYN (Figure 1B, red curve).

Impedimetric Aptasensor for Label-Free CYN Detection. For the impedimetric CYN detection, we employed the CYN9 aptamer sequence which exhibited a conformation change in the CD. Scheme 1 shows the steps of aptasensor fabrication which involve the formation of the self-assembled monolayer (SAM) from disulfide-modified aptamer on a gold surface. Then we employed the MCH blocking to minimize the nonspecific adsorption of the aptamers on the gold electrode by displacing the aptamer nucleotides from the Au surface[31] and ensure that the aptamer binds only from the sulfide moiety. This conformation will enhance the formation of the aptamer secondary structure for easy recognition of its ligand.

EIS is highly sensitive for surface modifications. The impedance-based aptasensor is commonly performed in the presence of negatively charged $[Fe(CN)_6]^{4-/3-}$ to record an increase in charge transfer resistance (R_{et}) due to the repulsion from negatively charged DNA aptamer. This is followed by a decrease or increase in R_{et} upon ligand recognition. For our case, the decrease of electron transfer resistance as a result of the conformational switching of the aptamer, which is induced by aptamer–CYN recognition was used as the aptasensor readout.

Scheme 1. Fabrication of the Label-Free Impedimetric Aptasensor for Cylindrospermopsin Based on Recognition-Induced Switching of the Aptamer

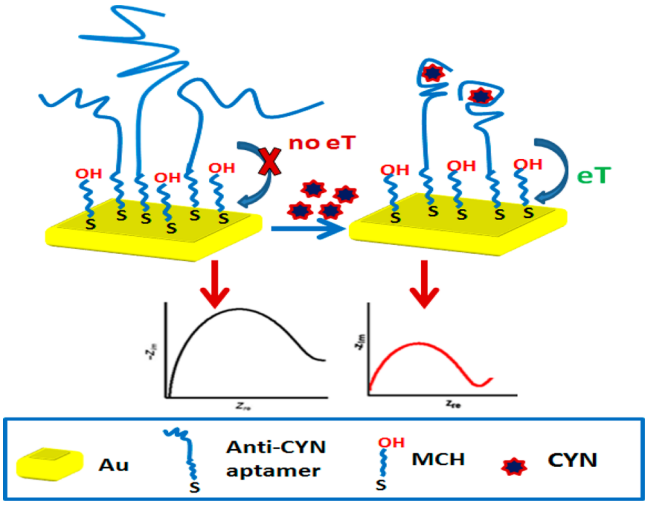

The monitoring of the aptasensor fabrication and its recognition of CYN were performed by recording the corresponding CV and EIS from PBS buffer containing 5 mM $[Fe(CN)_6]^{4-/3-}$, pH 7.4. For the CV analysis, a characteristic quasi-reversible voltammogram of the $[Fe(CN)_6]^{4-/3-}$ redox couple at a bare gold electrode with a peak separation ΔE_p of 88.8 mV is shown in Figure 2A (black curve). The electrochemical reaction is inhibited at the Au electrode after modification with anti-CYN aptamer, which is characterized by an increase in the peak separation of 532 mV and a substantial decrease in the peak current (Figure 2A, red curve). This could be attributed to the generation of a negatively charged interface from the negatively charged phosphate backbone of the DNA that repels the $[Fe(CN)_6]^{4-/3-}$ anions and retards the interfacial kinetics of the redox couple at the Au interface.

A further increase in the peak separation of 656 mV was observed after blocking the electrodes with MCH (Figure 2A, green curve). This reflects an additional decrease of the electron-transfer rate due to the backfilling of the uncovered sites on the gold surface. However, the typical CV behavior of

dx.doi.org/10.1021/ac502157g | Anal. Chem. XXXX, XXX, XXX–XXX

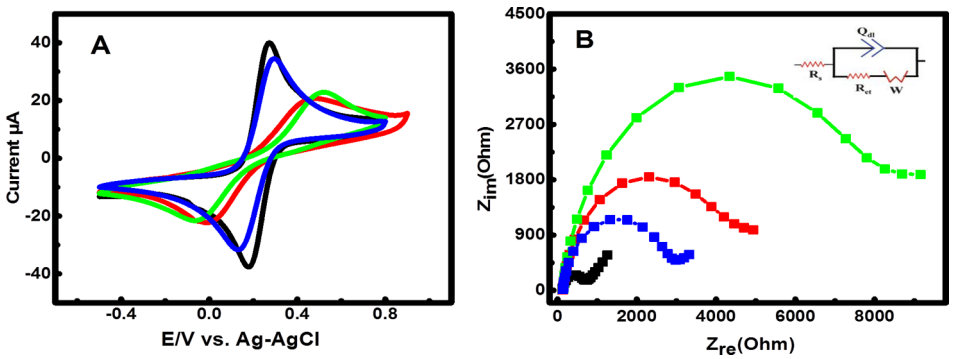

Figure 2. (A) Cyclic voltammograms (CVs) and (B) impedance spectra (Nyquist plots) of 5 mM $[Fe(CN)_6]^{4-/3-}$ in PBS, pH 7.4, for (a) bare Au electrode, (b) Au/CYN9, (c) Au/CYN9/MCH, and (d) after recognition to 60 nM CYN. The CV was performed at a scan rate of 100 mV/s, and the EIS parameters were in a frequency range of 10^5 to 3 Hz, a dc potential of +0.21 V, and an ac amplitude of 5 mV. The inset is the equivalent circuit used for the impedance data fitting.

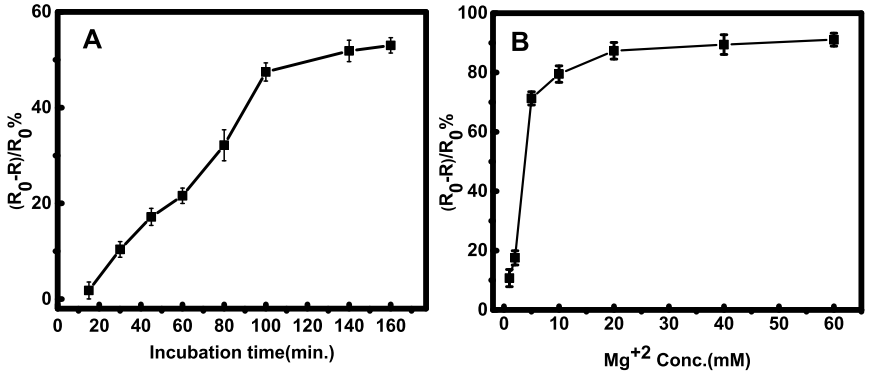

Figure 3. Effect of (A) the CYN incubation time and (B) Mg^{2+} concentration on aptasensor response for 60 nM CYN in 5 mM $[Fe(CN)_6]^{4-/3-}$ redox couple, 10 mM PBS (pH 7.4).

$[Fe(CN)_6]^{4-/3-}$ is almost recovered after the binding of 60 nM CYN to the aptamer modified electrode (Figure 2A, blue curve), implying greater accessibility of the redox couple to the aptasensor surface. The conformational change and folding of the CYN9 aptamer into a complex structure upon CYN recognition might be the reason for the recovered Faradaic process on the aptasensor surface.

For impedance measurements, Nyquist plots were used, which consists of a semicircle portion at high frequencies and a linear domain at lower frequencies corresponding to electron-transfer and diffusion-limited processes, respectively. The semicircle diameter can be quantified by fitting with a suitable model, such as the Randles-modified equivalent circuit (Figure 2B, inset)[32] as the electron transfer resistance (R_{et}) of the modified electrode surfaces. Thus, the diameter can be used to describe the interface properties of the electrode. Also, the circuit includes the solution resistance between working and reference electrodes R_s, Warburg impedance, Zw, resulting from the diffusion of ions to the interface from the bulk of the electrolyte and the constant phase element Q_{dl} (alternative to the double layer capacitance, C_{dl}), which relates directly to electrode roughness.

Figure 2B shows the Nyquist plots of various Au electrode modification process in the presence of equimolar $[Fe(CN)_6]^{4-/3-}$. Obviously, characteristic fast electron transfer and diffusion limiting processes were recorded on the bare gold electrode, which is reflected by a small semicircle diameter.

The assembly of a negatively charged disulfide anti-CYN aptamer onto the Au surface forms tightly packed films of aptamers that introduce a barrier to the interfacial electron transfer. This introduces an electrostatic repulsive force to the $[Fe(CN)_6]^{4-/3-}$ anions, thus enlarging the semicircle radius to R_{et} = 6334 Ω (red curve).

A further significant increase in R_{et} (7810 Ω) was observed after blocking with MCH due to the filling of the exposed free areas of the gold electrode, which reduces the accessibility of the redox couple to the electrode surface (Figure 2B, green curve). Upon recognition of the aptasensor to 60 nM CYN (Figure 2B, blue curve), a marked decrease of R_{et} (4780 Ω) was observed, which may originate from the change in the aptamer's conformation upon binding. This reflects the greater accessibility of the redox marker to the electrode surface (as proved from CD measurements). Such drop in the R_{et} is consistent with the CV behavior that is explained above and is likely to be due to the conformational change and folding of the aptamer to a structure of less exposed negative charges upon recognition of the toxin. This same decrease in R_{et}, which results from aptamer–target recognition has been previously reported.[33,34]

Aptasensor Optimization. The aptasensor's performance could be affected by some parameters such as the incubation time of aptasensor recognition to CYN. Figure 3A shows the responses of the aptasensors at different incubation times for 60 nM CYN solution. The sensor response $[(R_o - R)/R_o\ \%]$, which represents the percentage change in the R_{et} before and after binding, was used to evaluate the response. The sensor response increased slowly from 15 to 100 min, followed by a slight increase from 100 to 160 min, implying saturation of the

dx.doi.org/10.1021/ac502157g | Anal. Chem. XXXX, XXX, XXX–XXX

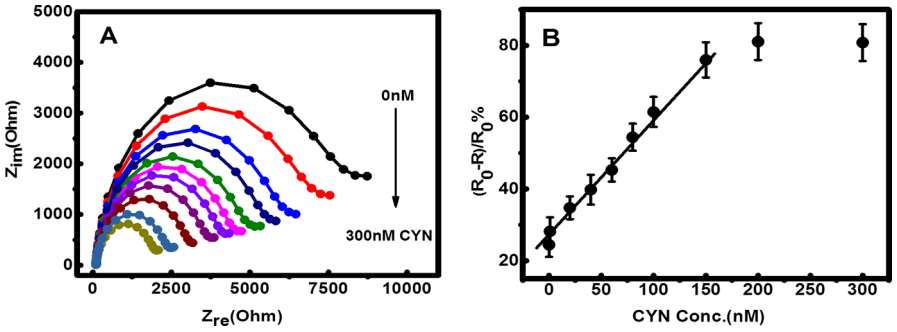

Figure 4. (A) Impedance measurements (Z_{im} vs Z_{re}, Nyquist plots) corresponding to the aptasensor to variable concentration of CYN of 0.00, 0.1, 1.0, 20, 40, 60, 80, 100, 150, 200 and 300 nM. (B) The calibration graph corresponding to $\Delta R/R_o$ % of aptasensor with CYN (nM). The error bars show the SD of three repetitive measurements. The conditions are as in Figure 2B.

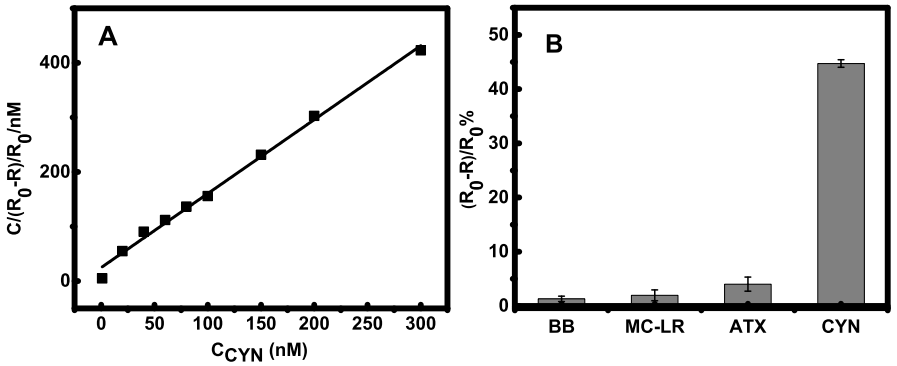

Figure 5. (A) Linearized Langmuir adsorption isotherm of CYN binding to anti-CYN aptamers anchored on gold electrodes. The line is the best linear fit to the experimental data from which the dissociation constant K_d was determined. (B) The aptasensor response $\Delta R/R_o$ % against binding buffer (BB), 1 nM of MC-LR, ATX, and CYN. The error bars represent the SD of three measurements.

aptamer modified electrode. Thus, 100 min was used as the optimum binding time in further experiments. Compared with other reported aptasensors of toxins, such as microcystin-LR,[33] 100 min as incubation time was relatively shorter.

DNA conformation can be controlled by the interaction with the metal ion, which stabilizes its secondary structure[35] and assists the formation of the ligand−aptamer complex. To investigate the role of Mg^{2+} for the structural conformation of the CYN9 aptamer and its recognition of CYN, binding buffers of various Mg^{2+} concentrations from 1 to 60 mM were used. The sensor response of $(R_0 - R)/R_0$ % was recorded for 60 nM CYN for all Mg^{2+} concentrations. As shown in Figure 3B, the maximum sensor response was observed at 20 mM Mg^{2+} with it then remaining constant up to 60 nM Mg^{2+}. Therefore, the binding buffer of 20 mM $MgCl_2$ was employed as a recognition buffer for further experiments.

Performance of the CYN Aptasensor. The aptasensor was used to record the impedimetric responses for various CYN concentrations. With increasing CYN concentration, the aptasensor records a decrease in the interfacial electron-transfer resistances, R_{et}. Thus, the R_{et} was used as the readout signal to quantify the recognizing analyte on the aptasensor surface.

Figure 4A shows the Nyquist plots of aptasensor for CYN at different concentrations of 0.1−300 nM. As depicted, there is substantial drop in the impedance response when the CYN concentration increases, due to the structural conformation change of the aptamer upon recognition with CYN.

The aptasensor exhibits a linear dependence on the CYN concentration as shown in a calibration plot, $[(R_o - R)/R_o$ %] versus CYN (Figure 4B), where CYN was easily detected at 100 pM, the limit of detection (LOD). The data for the calibration plot represented an average of three independent measurements with RSD of (2.0% to 9.0%), which indicates acceptable reproducibility of the aptasensor responses. The aptasensor LOD (0.039 μg/L) showed a comparable performance to the CYN commercial ELISA kit of LOD (0.040 μg/L). Moreover, for application in the field where CYN guideline value is 1 μg/L, the linear range of the aptasensor is fit for purpose.[8]

We then investigated how the binding affinity for CYN was affected by the anchoring of the disulfide-modified CYN aptamer onto the gold electrode. We employed the aptasensor response $(R_o - R)/R_o$ % to calculate the dissociation constant, K_d by considering a Langmuir isotherm,[36] which can be representative as a linearized equation as follows:

$$\frac{[\mathrm{CYN}]}{(\Delta R)} = \frac{[\mathrm{CYN}]}{(\Delta R)_{\max}} + \frac{K_d}{(\Delta R)_{\max}}$$

where $\Delta R = (R_0 - R)/R_0$, and $\Delta R_{max} = (R_0 - R_{max})/R_0$.

By neglecting the lower CYN concentration and plotting [CYN] versus [CYN]/ΔR as shown in Figure 5A, a linear plot with a regression coefficient of 0.996 was obtained. By dividing the y intercept by the slope, a K_d of (20.25 ± 2.7) nM is obtained. This is much lower than that obtained from the fluorescence assay for free aptamers in solution. Furthermore, the additional effect of the Mg^{2+} on the K_d was pronounced. The K_d of (20.25 ± 2.7) from 20 mM Mg^{2+} is lower than K_d (31.86 ± 9.7) nM from 2 mM Mg^{2+}. This result demonstrates the critical role of that cation on both the affinity of the aptamer and its conformational changes. The result is in agreement with

dx.doi.org/10.1021/ac502157g | Anal. Chem. XXXX, XXX, XXX−XXX

Table 2. Spike and Recovery Results (n = 3) Obtained from the CYN Aptasensor in Certified Sample (10 nM) and Tap Water

	CYN found (nM)		RSD%		recovery (%)	
CYN (nM)	certified CYN	tap H_2O	certified CYN	tap H_2O	certified CYN	tap H_2O
40	50.8 ± 4.9	41.3 ± 0.82	9.64	1.98	101.6	103.2
60	70.11 ± 3.3	57.5 ± 2.7	4.70	4.69	100.1	95.8
80	91.8 ± 1.95	82.25 ± 3.2	2.12	3.89	102	102.8

previous reports, which reveal that Mg^{2+} is involved in enhancing the binding affinity[37] and formation of the ligand−aptamer complex.

Specificity Studies. For practical applications, it is crucial to test the selectivity and the specificity of the CYN aptasensor in the presence of other interferences. To achieve this, two different control experiments were performed. First, 1 nM of coexistant cyanotoxins: anatoxin-a (ATX) and microcysitn-LR (MC-LR) were used. No obvious changes occur in the impedance response (change in the R_{et}) of the aptamer-functionalized electrode (Figure 5B). These results confirm the selectivity of aptasensor to CYN only. Moreover, the uracil, the moiety which was found in CYN structure was tested. Again, no significant change was observed in the impedance signals (data not shown). Third control experiment was performed to ensure that CYN did not bind to other aptamer sequences. Disulfide-derivatized aptamer [HO-$(CH_2)_6$S−S-$(CH_2)_6$-DNA], which does not bind to CYN was immobilized, and the sensor response was recorded. No significant difference in the impedance response could be observed (data not shown), implying that the DNA-modified Au electrode did not recognize or form a complex with CYN.

Analysis of Real Samples. The performances of aptasensor for the quantification of CYN in real samples was tested by spiking different amounts of CYN into certified and tap water samples. The results are summarized in Table 2. The recoveries which were calculated from the standard plot in BB for the two samples ranged from 100.1% to 102% and 95.8% to 103.2%, respectively. The relative deviations were between 2.12% and 9.64%, indicating acceptable accuracy.

CONCLUSIONS

In this work, we have successfully developed DNA aptamers that bind CYN with high selectivity and high affinity for the fabrication of a label-free impedimetric aptasensor for CYN. The identified aptamers show high affinity with dissociation constants values in the nanomolar range, which is excellent for small toxin like CYN (415.43 Da). The aptamer sequence that exhibited a conformational change upon toxin binding according to the results of the CD spectra was used to design a label-free impedance based aptasensor. The aptasensor was based on the decrease of electron transfer resistance that was observed upon the binding of the CYN ligand. Fluorescence and impedance assays were used to calculate the dissociation constant, and a lower K_d value was obtained from the aptasensor response, reflecting that aptamer disulfide modification or surface immobilization improved the aptamer affinity to the CYN. The effect of Mg^{2+} on the recognition of CYN by the aptamer-modified electrodes was studied and a lower K_d value found reflecting the enhanced affinity. The developed aptasensor showed a low LOD (100 pM) with a wide linear range of 0.1 to 80 nM. Cross-reactivity studies proved that the aptasensor had very good selectivity against other cyanobacterial toxins ATX and MC-LR. In summary, we believe that electrochemical-based aptasensors can provide alternatives for the sensitive monitoring of toxins for water quality control and environmental safety.

ASSOCIATED CONTENT

Supporting Information

Additional information as noted in text. This material is available free of charge via the Internet at http://pubs.acs.org.

AUTHOR INFORMATION

Corresponding Author

*E-mail: m.zourob@cranfield.ac.uk. Tel: +44 (0) 1234 758318.

Notes

The authors declare no competing financial interest.

REFERENCES

(1) Bourke, A. T. C.; Hawes, R. B.; Neilson, A.; Stallman, N. D. *Toxicon* **1983**, *21* (1983), 45−48.
(2) Falconer, I. R.; Humpage, A. R. *Environ. Toxicol.* **2006**, *4*, 299−304.
(3) Schembri, M. A.; Neilan, B. A.; Saint, C. P. *Environ. Toxicol.* **2001**, *16*, 413−421.
(4) Norris, R. L.; Eaglesham, G. K.; Pierens, G.; Shaw, G. R.; Smith, M. J.; Chiswell, R. K.; Seawright, A. A.; Moore, M. R. *Environ. Toxicol.* **1999**, *14*, 163−165.
(5) Griffiths, D. J.; Saker, M. L. *Environ. Toxicol.* **2003**, *18*, 78−93.
(6) Looper, R. E.; Runnegar, M. T. C.; Williams, R. M. *Angew. Chem., Int. Ed.* **2005**, *44*, 3879−3881.
(7) Banker, R.; Carmeli, S.; Werman, M.; Teltsch, B.; Porat, R.; Sukenik, A. *J. Toxicol. Environ. Health, Part A* **2001**, *62*, 281−288.
(8) Humpage, A. R.; Falconer, I. R.; Humpage, A. R. *Environ. Toxicol.* **2003**, *18*, 94−103.
(9) Hawkins, P. R.; Runnegar, M. T.; Jackson, A. R.; Falconer, I. R. *Appl. Environ. Microbiol.* **1985**, *50*, 1292−1295.
(10) Bazin, E.; Huet, S.; Jarry, G.; Hegarat, L. L.; Munday, J. S.; H.A, R.; Fessard, V. *Environ. Toxicol.* **2012**, *27*, 277−284.
(11) Svrcek, C.; Smith, D. W. *J. Environ. Eng. Sci.* **2004**, *3*, 155−185.
(12) Li, R.; Carmichael, W. W.; Brittain, S.; Eaglesham, G. K.; Shaw, G. R.; Mahakhant, A.; Noparatnaraporn, N.; Yongmanitchai, W.; Kaya, K.; Watanabe, M. M. *Toxicon* **2001**, *39*, 973−980.
(13) *Algal Toxins in Seafood and Drinking Water*; Falconer, I. R., Ed.; Academic Press: London, 1993.
(14) Welker, M.; Bickel, H. *Water Res.* **2002**, *36*, 4659−4663.
(15) Kubo, T.; Sanob, T.; Hosoya, K.; Tanaka, N.; Kaya, K. *Toxicon* **2005**, *46*, 104−107.
(16) Vasas, G.; Gáspár, A.; Páger, C.; Surányi, G.; Máthé, C.; Hamvas, M. M.; Borbely, G. *Electrophoresis* **2004**, *25*, 108−115.
(17) Bláhová, L.; Oravec, M.; Maršálek, B.; Šejnohová, L.; Šimek, Z.; Bláha, L. *Toxicon* **2009**, *53*, 519−524.
(18) Elliott, C. T.; Redshaw, C. H.; George, S. E.; Campbell, K. *Harmful Algae* **2013**, *24*, 10−19.
(19) Tuerk, C.; Gold, L. *Science* **1990**, *249* (4968), 505−510.
(20) Ellington, A. D.; Szostak, J. W. *Nature* **1990**, *346* (6287), 818−822.
(21) Hu, R.; Wen, W.; Wang, Q.; Xiong, H.; Zhang, X.; Gu, H.; Wang, S. *Biosens. Bioelectron.* **2014**, *53*, 384−389.
(22) Dong, Z.-M.; Zhao, G.-C. *Sensors* **2012**, *12*, 7080−7094.
(23) He, P.; Liu, L.; Qiao, W.; Zhang, S. *Chem. Commun.* **2014**, *50*, 1481−1484.

(24) Cruz-Aguado, J. A.; Penner, G. J. *Agric. Food Chem.* **2008**, *56*, 10456−10461.
(25) McKeague, M.; Bradley, C. R.; De Girolamo, A.; Visconti, A.; Miller, J. D.; DeRosa, M. C. *Int. J. Mol. Sci.* **2010**, *11*, 4864−4881.
(26) Handy, S. M.; Yakes, B. J.; DeGrasse, J. A.; Campbell, K.; Elliott, C. T.; Kanyuck, K. M.; DeGrasse, S. L. *Toxicon* **2013**, *61*, 30−37.
(27) Nakamura, C.; Kobayashi, T.; Miyake, M.; Shirai, M.; Miyakea, J. *Mol. Cryst. Liq. Cryst.* **2001**, *371*, 369−374.
(28) Simossis, V. A.; Kleinjung, J.; Heringa, J. *Nucleic Acids Res.* **2005**, *33*, 816−824.
(29) Stoltenburg, R.; Reinemann, C.; Strehlitz, B. *Biomol. Eng.* **2007**, *24*, 381−403.
(30) Nelson, H.C. M.; Finch, J. T.; Luisi, B. F.; Klug, A. *Nature* **1987**, *325*, 821−823.
(31) Liu, Y.; Zhou, Q.; Revzin, A. *Analyst* **2013**, *138*, 4321−4326.
(32) Vyas, R. N.; Li, K.; Wang, B. *J. Phys. Chem. B* **2010**, *114*, 15818−15824.
(33) Linn, Z.; Huang, H.; Xu, Y.; Gao, X.; Qiu, B.; Chen, X.; Chen, G. *Talanta* **2013**, *103*, 371−374.
(34) Dua, Y.; Lia, B.; Wang, F.; Dong, S. *Biosens. Bioelectron.* **2009**, *24*, 1979−1983.
(35) Deng, Q.; Watson, C. J.; Kennedy, R. T. *J. Chromatogr. A* **2003**, *1005*, 123−130.
(36) Steel, A. B.; Herne, T. M.; Tarlov, M. J. *Bioconjugate Chem.* **1999**, *10*, 419−423.
(37) Muller, M.; Weigand, J. E.; Weichenrieder, O.; Suess, B. *Nucleic Acids Res.* **2006**, *34*, 2607−2617.